Enhancing Fuel-Cell Longevity via Multi-Objective Dynamic Programming

A. Genidy, M. Léau, D. Nelson-Gruel, A. Ketfi-Chérif, D. Von-Wissel, Guillaume Colin

Enhancing Fuel-Cell Longevity via Multi-Objective Dynamic Programming ⋆

A. Genidy [*,**] **M. Léau** [**] **D. Nelson-Gruel** [**] **A. Ketfi-Chérif** [*]
D. Von-Wissel [*] **G. Colin** [**]

[*] *Ampere sas, 78084 Guyancourt, France (e-mails: abdelrahman.genidy@ampere.cars).*
[**] *University of Orléans–INSA-CVL, PRISME UR4229, Orléans, France.*

Abstract: Proton-exchange-membrane fuel cells are emerging as a key technology for clean electric vehicles. However, degradation mechanisms arising from operating conditions hinder the market entry of fuel cell electric vehicles. Therefore, an energy management strategy is crucial to optimize fuel-cell operation while minimizing both degradation and hydrogen consumption. Accordingly, this paper proposes a two-state multi-objective dynamic programming approach to address this problem. Compared to the conventional approach that considers only hydrogen consumption, the simulation results reveal a significant reduction of 98.38% in fuel-cell degradation, accompanied by a slight increase in fuel consumption. This reduction in fuel-cell degradation is achieved by limiting start-stop cycles and transient loading on the fuel-cell stack.

Keywords: Fuel Cell Hybrid Electric Vehicles (FCHEVs), Dynamic Programming (DP), Energy Management Strategy (EMS), Health-Conscious EMS, Optimal Control Problem (OCP), Proton-Exchange-Membrane Fuel Cell (PEMFC), PEMFC Degradation

1. INTRODUCTION

Nowadays, automotive manufacturers and research institutes are devoted to promoting alternative energy sources to accelerate the shift towards clean, efficient, and affordable electric traction systems (Sulaiman et al., 2018). With the gradual maturation of fuel-cell (FC) technology, FC hybrid electric vehicles (FCHEVs) are becoming a promising substitute for internal-combustion-engine (ICE) vehicles and ICE-based hybrid electric vehicles (HEVs) due to their zero emissions, good driving range, and quick refueling (Yue et al., 2019). Among various FC types, the proton-exchange-membrane fuel cell (PEMFC) is distinguished by its high power density, high efficiency, and low operating temperature, which make it suitable for vehicle applications (Alyakhni et al., 2021).

Owing to the poor dynamic response of PEMFCs, FCHEVs are equipped with auxiliary energy sources, such as batteries or supercapacitors, to support fast transient response and store regenerated energy (Teng et al., 2020). Hence, an Energy Management Strategy (EMS) is required to allocate power among these sources, minimize hydrogen consumption, and meet the vehicle's operating constraints (Fletcher et al., 2016). Moreover, as PEMFC stacks are costly and degrade over time, designing a health-conscious EMS that considers PEMFC durability is crucial to avoid increasing the operating costs of the electric vehicle (EV) (Sulaiman et al., 2018).

⋆ This paper is supported by a CIFRE contract with the "Association Nationale de la Recherche et de la Technologie" (ANRT). It is also developed within a collaborative framework between Ampere sas, and PRISME laboratory.

Energy management strategies are typically classified into rule-based and optimization-based methods. Rule-based methods are convenient for real-time applications, such as FCHEVs, as they can employ simple rules to manage multiple energy sources. However, their reliance on human intuition, engineering expertise, and expert knowledge limits their ability to ensure optimal performance under varying conditions. (Zhang et al., 2015).
In contrast, optimization-based methods improve performance by formulating the energy management task as a mathematical optimization problem. The optimal control sequence is derived by minimizing an objective function without violating the system constraints. These methods are categorized into global and local approaches (Zhang et al., 2015). Local approaches address the problem by defining an instantaneous cost function that is updated over time, enabling them to overcome computational limitations, and making them adequate for FCHEVs. However, they do not achieve global optimality. Therefore, global approaches are often used as benchmarks to evaluate local approaches performance, as they achieve global optimality.

Most studies on global approaches focus solely on minimizing fuel consumption. Few have addressed the trade-off between the FC's state of health and hydrogen economy. Dynamic programming (DP) is commonly employed in this context to optimize the operating costs of FCHEVs. For instance, Hu et al. (2016) proposed a DP-based EMS to minimize FC degradation by using its equivalent hydrogen consumption as part of the cost function. Their result was validated on a fuel-cell city bus, achieving a good balance between fuel economy and system durability. The same cost function was employed in another multi-dimensional DP proposed by (Liu et al., 2022) during

their attempt to improve the computational efficiency of the DP algorithm while maintaining its accuracy. In their work, hydrogen consumption was reduced by 3.10%, while FC and battery durability improved by 1.08% and 0.13%, respectively. Moratti et al. (2024) introduced a two-state DP that constrains the FC current ramp rate and shutdowns to enable operation under minimal degradation conditions and higher efficiency. Simulation results showed that introducing limitations on the FC current variation and shutdowns slightly affects energy consumption but significantly reduces FC aging.

In prior DP literature, some research focuses on modifying the DP algorithm to improve its efficiency and accuracy, using the FC degradation problem as a case study rather than properly modeling the cost function. Other researchers indirectly minimize FC degradation by limiting the loading conditions that accelerate the degradation process or by targeting equivalent hydrogen consumption to degradation. Therefore, in this work, a two-state dynamic programming model is proposed to directly incorporate FC degradation and loading decisions as minimization criteria within a weighted multi-objective cost function. The weights of the employed cost function are determined based on a Pareto front analysis.

This paper is organized as follows: Section 2 describes the architecture of a FCHEV powertrain, presenting the propulsion system model and the FC degradation model. Section 3 introduces the proposed DP-based energy management strategy. Section 4 discusses the simulation results, and section 5 provides the conclusion.

2. POWERTRAIN STRUCTURE AND MODELISATION

This study adopts a parallel architecture for a FC/battery propulsion system (Liu et al., 2022). In this configuration, an electric machine powers the EV using a hybrid power source composed of a Li-ion battery and a PEMFC system. Through an oxidation-reduction reaction between hydrogen and oxygen, the PEMFC converts chemical energy into electrical energy. Therefore, a unidirectional DC-DC converter is installed on the PEMFC side to regulate its current flow into the DC bus, while the battery system is directly connected to maintain the DC bus voltage.

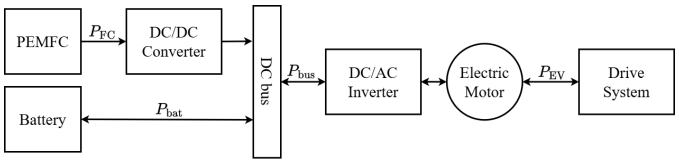

Fig. 1. Considered FC/battery powertrain configuration

When the EV's power demand is specified, the output power from the PEMFC and the battery jointly respond to meet the power requirements for both propulsion and regenerative braking. Specifically, the deviation between the power requested by the DC/AC inverter and the power supplied by the PEMFC is compensated by the battery.

$$P_{\text{bus}}(k) = P_{\text{FC}}(k) \cdot \eta_{\text{DC/DC}} + P_{\text{bat}}(k) \tag{1}$$

P_{bus} denotes the bus power demand of the inverter that provides power to drive the electric machine. Its value is calculated using (2). In addition, P_{FC}, P_{bat}, and $\eta_{\text{DC/DC}}$ express the FC power, battery power and DC/DC converter efficiency, respectively.

$$P_{\text{bus}}(k) = P_{\text{EV}}(k) \cdot \left(\eta_{\text{DC/AC}} \cdot \eta_{\text{motor}}\right)^{-\text{sign}(P_{\text{EV}}(k))} \tag{2}$$

$\eta_{\text{DC/AC}}$ is the inverter efficiency, and η_{motor} is the electric machine efficiency. All powertrain components are assumed to be lossless and will be updated in future work.

2.1 Vehicle Model

The vehicle propulsion power P_{EV} is calculated through the vehicle's longitudinal dynamics presented in (3 - 8). The vehicle traction force F_{tra} is formulated as the sum of aerodynamic resistance F_{a}, rolling friction F_{r}, inertial resistance F_{acc}, and gradient resistance F_{g} caused by gravity when driving on a sloping road.

$$P_{\text{EV}}(k) = F_{\text{tra}}(k) \cdot V_{\text{EV}}(k) \tag{3}$$
$$F_{\text{tra}}(k) = F_{\text{a}}(k) + F_{\text{r}}(k) + F_{\text{acc}}(k) + F_{\text{g}}(k) \tag{4}$$
$$F_{\text{a}}(k) = 0.5 \cdot \rho \cdot A \cdot C_x \cdot v_{EV}^2(k) \tag{5}$$
$$F_{\text{r}}(k) = m \cdot g \cdot (C_0 + C_1 \cdot v_{EV}^2(k)) \cdot \cos(\theta(k)) \tag{6}$$
$$F_{\text{acc}}(k) = m \cdot a_{EV}(k) \tag{7}$$
$$F_g(k) = m \cdot g \cdot \sin(\theta(k)) \tag{8}$$

where ρ is the air density, A is the vehicle frontal surface, C_x is the air drag coefficient, m the vehicle mass, g is the gravitational acceleration, v_{EV} and a_{EV} are the speed and acceleration of the vehicle, C_0 & C_1 are the coefficients of the rolling resistance, and θ is the road slope angle.

Table 1. Parameters of electric vehicle model

A (m^2)	ρ (kg/m^3)	C_x	C_1 (s^2/m^2)	C_0	θ (°)
2.75	1.2	0.3	$1.6 \cdot 10^{-6}$	0.008	0

2.2 Fuel-Cell-Stack Model

To describe the PEMFC stack voltage, a typical polarization curve is used (Bressel et al., 2016), expressed below based on both experimental and mathematical derivations.

$$V_{\text{st}}(k) = n\left(E_0 - R \cdot J(k) - A \cdot \ln\left(\frac{J(k)}{i_0}\right) - B \cdot \ln\left(1 - \frac{J(k)}{i_L}\right)\right) \tag{9}$$

$$P_{\text{FC}}(k) = V_{\text{st}}(k) \cdot I_{\text{FC}}(k) \tag{10}$$

where V_{st}, n, J, A, B, I_{FC} and P_{FC} are the stack voltage, number of cells, current density, tafel constant, concentration constant, FC current, and FC power, respectively.

Table 2. Parameters of PEMFC stack model

n	A (V)	B (V)	A_{cell} (cm^2)	$P_{\text{FC}_{\max}}$ (kW)
60	$2.309 \cdot 10^{-2}$	-0.4831	100	36

To identify the missing parameters of the aforementioned model, the Levenberg–Marquardt optimization algorithm is used to fit the model to PEMFC experimental data measured by FCLAB. This data was published as part of the IEEE Prognostics and Health Management (PHM) 2014 Data Challenge (Harel, 2021).

Table 3. Estimated PEMFC model parameters

E_0 (V)	R ($\Omega \cdot cm^2$)	i_0 (A/cm^2)	i_L (A/cm^2)
1	0.1809	$2.16 \cdot 10^{-6}$	55.1

where E_0, R, i_0, and i_L are the open circuit voltage, total specific resistance, exchange current density, and limiting

current density, respectively.
The tested PEMFC stack by FCLAB consists of five cells, with nominal and maximum current densities of 0.7 and 1 A/cm^2, respectively. In our work, we adopted the same PEMFC stack, adjusting its specifications to include 60 cells and to meet the power requirements of our EV.

2.3 Hydrogen Consumption Model

During the PEMFC operation, the instantaneous hydrogen consumption rate $\dot{m}_{\mathrm{H_2}}$ can be calculated as a function of FC power and efficiency η_{FC} (Song et al., 2020).

$$\dot{m}_{\mathrm{H_2}}(k) = \frac{P_{\mathrm{H_2}}}{LCV_{\mathrm{H_2}}} = \frac{P_{\mathrm{FC}}(k)}{LCV_{\mathrm{H_2}} \cdot \eta_{\mathrm{FC}}(k)} \tag{11}$$

where $LCV_{\mathrm{H_2}}$ is the lower calorific value of hydrogen, with a value of 120,000 J/g. It represents the amount of energy released when hydrogen is burned, excluding the latent heat of vaporization of the water produced during combustion.

Before calculating hydrogen consumption, it is essential to determine the efficiency of the PEMFC system. In this paper, we calculate the efficiency by using a curve that directly relates FC current I_{FC} to its efficiency. Due to the lack of FC dataset in the literature, we use an approximate efficiency curve to generate the hydrogen consumption curve shown in Fig. 2.

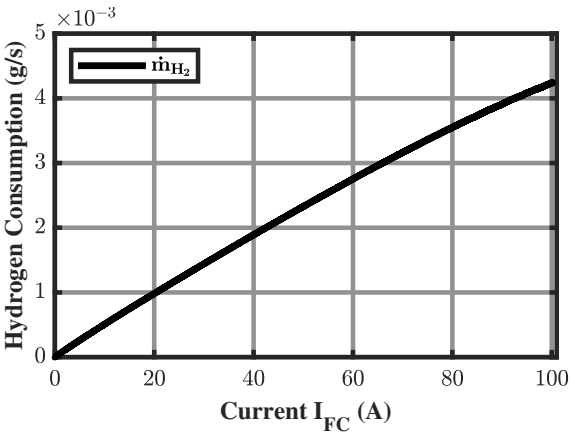

Fig. 2. PEMFC hydrogen consumption curve

To sum up, once the FC current I_{FC} is known, the instantaneous hydrogen consumption rate can be calculated, which becomes the first instantaneous cost function L_1 to be minimized using dynamic programming.

2.4 PEMFC Aging Model

PEMFC performance degradation is defined as the voltage drop that occurs when the FC keeps operating at its maximum current (Pei et al., 2008). This voltage drop $\Delta V_{\mathrm{FC_{deg}}}$ results from the diverse operating conditions.

$$\Delta V_{\mathrm{FC_{deg}}}(k) = K_{\mathrm{c}} \cdot \left(\Delta V_{\mathrm{load}}(k) + \beta \cdot \frac{\Delta k}{3600} \right) \tag{12}$$

where ΔV_{load} is the instantaneous degradation caused by the FC load current. On the contrary, β is the FC natural decay rate due to catalyst degradation, membrane wear, electrode corrosion, and gas diffusion layer damage. In addition, K_{c} is a correction coefficient to compensate for the differences between in-laboratory and on-road results.

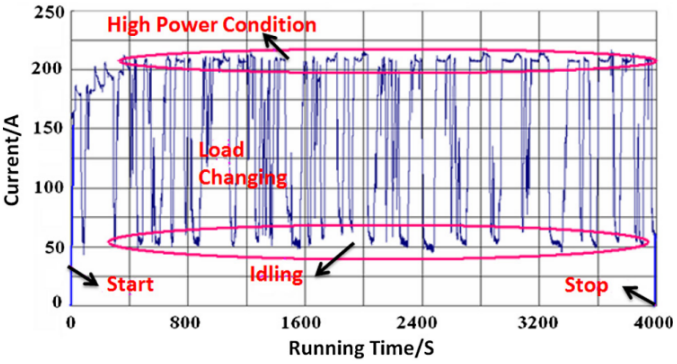

Fig. 3. An example of PEMFC loading conditions (Chen et al., 2015)

Furthermore, FC loading conditions are classified into four categories: start-stop, load-changing, low-load (idling), and high-load, as shown in Fig. 3. Accordingly, the FC degradation, caused by the applied load current, is evaluated by adding the corresponding voltage degradation for each loading condition, where ΔV_{SS}, ΔV_{LC}, ΔV_{LL}, and ΔV_{HL} represent, respectively, the FC voltage drop induced by start-stop cycles, load change, low load, and high load.

$$\begin{aligned} \Delta V_{\mathrm{load}}(k) &= \Delta V_{\mathrm{SS}}(k) + \Delta V_{\mathrm{LC}}(k) + \Delta V_{\mathrm{LL}}(k) + \Delta V_{\mathrm{HL}}(k) \\ &= r_1 + r_2 \cdot \frac{|\Delta P_{\mathrm{FC}}(k)|}{1000} + r_3 \cdot \frac{\Delta k}{3600} + r_4 \cdot \frac{\Delta k}{3600} \end{aligned} \tag{13}$$

Table 4 details the degradation rate for each load category, with their experimental values derived from bench-testing results reported by Fletcher et al. (2016).

Table 4. PEMFC degradation rates (per cell)

Parameter	Value	Description
r_1	23.91 [μV/cycle]	Start-stop degradation rate
r_2	0.0441 [μV/ΔkW]	Load-change degradation rate
r_3	10.17 [μV/h]	Low-load degradation rate
r_4	11.74 [μV/h]	High-load degradation rate
β	0 [μV/h]	Natural decay rate
K_{c}	1	Correction coefficient
V_{BOL}	0.6 [V]	Maximum supplied volt at the beginning of life

To be more specific, only one degrading factor is detected at each time step k. In other words, start-stop degradation ΔV_{SS} is realized each time the FC is activated. Low-load conditions ΔV_{LL} are defined when the PEMFC output power is less than or equal to 20% of its maximum power $P_{\mathrm{FC}}^{\max}$. Similarly, high-load degradation ΔV_{HL} is identified when FC power exceeds 80% of its maximum value $P_{\mathrm{FC}}^{\max}$. As for other degrading elements, the voltage degradation per kW ΔV_{LL} is determined during transient load changes. Hence, the FC degradation is computed instantaneously at every step k to be minimized by dynamic programming as a second instantaneous cost function L_2.

$$\Delta V_{\mathrm{load}}(k) = \begin{cases} \Delta V_{\mathrm{SS}}(k), & \text{if on/off triggered} \\ \Delta V_{\mathrm{LL}}(k), & \text{if } 0 < P_{\mathrm{FC}}(k) \leq 0.2 \cdot P_{\mathrm{FC}}^{\max} \\ \Delta V_{\mathrm{HL}}(k), & \text{if } P_{\mathrm{FC}}(k) \geq 0.8 \cdot P_{\mathrm{FC}}^{\max} \\ \Delta V_{\mathrm{LC}}(k), & \text{if } |\Delta P_{\mathrm{FC}}(k)| > 0 \\ 0, & \text{otherwise} \end{cases} \tag{14}$$

To calculate the PEMFC lifetime, its end-of-life voltage degradation is set at 10% of the initial maximum supplied

voltage. This threshold is recommended by various FC manufacturers as a critical limit. Using this threshold and the duration N of the EV's drive cycle in seconds, the FC's potential lifespan is estimated by (Pei et al., 2008):

$$T_{\mathrm{FC}} = \frac{10\% \cdot V_{\mathrm{BOL}} \cdot N}{\left(\sum_{t=1}^{N-1} V_{\mathrm{FC_{deg}}}(k) \cdot 10^{-6}\right) \cdot 3600} \tag{15}$$

It is worth noting that the result obtained from this model is just an estimation, influenced by the degradation rates attained from the literature for various PEMFCs.

2.5 Battery Model

For the Li-ion battery, an internal resistance-based model is employed to characterize the electric performance of the battery pack. The model consists of an internal resistor R_{int} and an open circuit voltage U_{OC} connected in series.

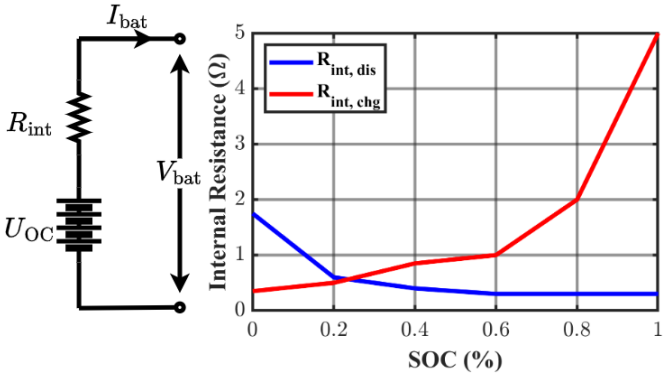

Fig. 4. R_{int} versus battery state of charge (SOC)

According to Kirchhoff's law, the battery voltage V_{bat} can be calculated as a function of SOC and current I_{bat}.

$$V_{\mathrm{bat}}(k) = U_{\mathrm{OC}}(SOC(k)) - R_{\mathrm{int}}(SOC(k)) \cdot I_{\mathrm{bat}}(k) \tag{16}$$

The open-circuit voltage U_{OC} and internal resistance R_{int} depend on SOC. These functions are provided by battery suppliers, as shown in Fig. 4. The battery power P_{bat} is then estimated by multiplying (16) by the current.

$$P_{\mathrm{bat}}(k) = U_{\mathrm{OC}}(SOC(k)) \cdot I_{\mathrm{bat}}(k) - I_{\mathrm{bat}}^2(k) \cdot R_{\mathrm{int}}(SOC(k)) \tag{17}$$

After solving (17), the battery current can be calculated as a function of the battery power.

$$I_{\mathrm{bat}}(k) = \frac{U_{\mathrm{OC}}(SOC(k)) - \sqrt{U_{\mathrm{OC}}^2(SOC(k)) - 4 \cdot R_{\mathrm{int}}(SOC(k)) \cdot P_{\mathrm{bat}}(k)}}{2 \cdot R_{\mathrm{int}}(SOC(k))} \tag{18}$$

Relying on the calculated current, the SOC of the battery is defined by (19) as a percentage indicator of the remaining battery capacity versus its nominal one.

$$SOC(k) = SOC(k_0) - \eta_{bat} \frac{I_{\mathrm{bat}}(k) \cdot \Delta k}{Q_{\mathrm{bat}}} \tag{19}$$

where Q_{bat} and η_{bat} denote the nominal capacity of the battery pack and the battery charge/discharge efficiency. The studied battery has a capacity of 28 Ah.

3. MULTI-OBJECTIVE DYNAMIC PROGRAMMING

To minimize hydrogen consumption and extend PEMFC lifetime over a given driving cycle, DP is applied to find the optimal power split between the battery and PEMFC.

$$J = \sum_{k=0}^{N-1} W_1 \cdot \dot{m}_{\mathrm{H_2}}(x_{2_k}) + W_2 \cdot \Delta V_{\mathrm{FC_{deg}}}(u_k, x_{2_k}) \tag{20}$$

W_1 and W_2 are weighting coefficients for the two components of the cost function. These weights are included to provide flexibility in meeting different design requirements.

To obtain the optimal battery SOC trajectory, the SOC is proposed as a state variable for the DP algorithm. Simultaneously, FC current (I_{FC}) is introduced as a second state variable to manage PEMFC performance and its consumption. Additionally, the control variable is defined as the variation in FC current (ΔI_{FC}) to help mitigate excessive fluctuations and limit their impact on FC aging.

$$u_k = \Delta I_{\mathrm{FC}}(k), \quad \boldsymbol{x}_k = \begin{bmatrix} x_{1_k} \\ x_{2_k} \end{bmatrix} = \begin{bmatrix} SOC(k) \\ I_{\mathrm{FC}}(k) \end{bmatrix}$$

The SOC is discretized into 101 points on the DP grid with 1% steps, while the current grid has 201 points, each corresponding to a 0.5 A step. A maximum absolute current rate of 10 A/s is set, with the control input grid discretized into 201 points, with 0.1 A/s steps. This 10 A/s limit is decided based on manufacturers' recommendations to prevent critical loading that could damage the stack.

$$x_{1_k} \in [0, 1], \quad x_{2_k} \in [0, 100], \quad u_k \in [-10, 10]$$

Moreover, min-max normalization is applied to the two components of the cost function, which have different orders of magnitude, to ensure a balanced contribution from each objective during optimization.

$$\tilde{J} = \sum_{k=0}^{N-1} \tilde{W}_1 \cdot \tilde{L}_1(x_{2_k}) + \tilde{W}_2 \cdot \tilde{L}_2(u_k, x_{2_k}) \tag{21}$$

$$\tilde{W}_1 \in [0, 1], \quad \tilde{W}_2 \in [0, 1], \quad \tilde{W}_1 + \tilde{W}_2 = 1$$

In min-max normalization, data is scaled to a fixed range, typically $[0, 1]$, by subtracting the minimum value and dividing by the data range. In our case, maximum hydrogen consumption ($\dot{m}_{\mathrm{H_2,max}}$) occurs as the FC operates at maximum load current, while the minimum consumption ($\dot{m}_{\mathrm{H_2,min}}$) is zero. Similarly, maximum FC degradation ($\Delta V_{\mathrm{FC_{deg,max}}}$) corresponds to one start-stop cycle degradation and its minimum ($\Delta V_{\mathrm{FC_{deg,min}}}$) value is zero.

$$\tilde{L}_1(x_{2_k}) = \frac{\dot{m}_{\mathrm{H_2}}(x_{2_k}) - \dot{m}_{\mathrm{H_2,min}}}{\dot{m}_{\mathrm{H_2,max}} - \dot{m}_{\mathrm{H_2,min}}} \tag{22}$$

$$\tilde{L}_2(u_k, x_{2_k}) = \frac{\Delta V_{\mathrm{FC_{deg}}}(u_k, x_{2_k}) - \Delta V_{\mathrm{FC_{deg,min}}}}{\Delta V_{\mathrm{FC_{deg,max}}} - \Delta V_{\mathrm{FC_{deg,min}}}} \tag{23}$$

Finally, the optimization problem for determining the optimal control policy for the FCHEV is formulated as the following discrete-time control problem:

$$\min_{u_k} \tilde{J} \tag{24}$$

where the model equations can be summarized as follows:

$$x_{1_{k+1}} = f(x_{2_k}) + x_{1_k} \tag{25}$$

$$x_{2_{k+1}} = u_k + x_{2_k} \tag{26}$$

To ensure the safe and smooth operation of the FC and battery, constraints related to their safety ratings and the power flow between them must be satisfied.

$$0.2 \leq x_{1_k} \leq 0.8 \tag{27}$$

$$0 \leq x_{2_k} \leq 100 \tag{28}$$

$$I_{\mathrm{chg,max}} \leq I_{\mathrm{bat}}(k) \leq I_{\mathrm{dis,max}} \tag{29}$$

$$4 \cdot R_{\mathrm{int}}(k) \cdot P_{\mathrm{bat}}(k) \leq U_{\mathrm{OC}}^2(k) \tag{30}$$

where the maximum battery charge ($I_{\mathrm{chg,max}}$) and discharge ($I_{\mathrm{dis,max}}$) current are -125 A and 100 A, respec-

tively. These values are obtained from the battery manufacturer. The final SOC is constrained to match or exceed the initial SOC to secure a charge-sustaining behaviour.

$$x_{1_N} \geq x_{1_0} \tag{31}$$

4. SIMULATION RESULTS

The DP algorithm produces a multi-dimensional lookup table that specifies the optimal control action for each combination of the two states (x_1 & x_2) (Bertsekas, 2005). This lookup table can be directly implemented in a forward simulation model, which runs in a time loop from the beginning to the end of the problem. At each time step in the forward simulation, the optimal policy from the lookup table is applied, and the corresponding optimal cost is computed. This process ultimately determines the entire optimal system trajectory. To examine the impact of driving patterns on the optimization results, the Worldwide Harmonized Light Vehicle Test Procedure (WLTP) is used in the forward simulation, with a 1-second sampling interval (Δk).
Before realizing the optimal energy management strategy, Pareto front analysis is conducted to derive the weights for the two cost functions, achieving the optimal compromise.

4.1 Trade-off between FC Degradation and H_2 Consumption

The degradation weight ($\tilde{W}_2$) is designed to range from 0 to 1, while the consumption weight ($\tilde{W}_1$) complements it, ensuring their sum equals 1. In this way, the Pareto front represents the trade-off between the two objectives, with each point on the front corresponding to a different weight combination.

$$\tilde{W}_2 \in \begin{cases} \{0, 0.1, 0.2, \ldots, 0.9\}, & 0 \leq \tilde{W}_2 \leq 0.9 \\ \{0.91, 0.92, \ldots, 1\}, & 0.9 < \tilde{W}_2 < 1 \end{cases}, \quad \tilde{W}_1 = 1 - \tilde{W}_2$$

when ($\tilde{W}_2 = 0$), DP is solely concerned with minimizing hydrogen consumption. On the other hand, FC degradation is the only cost function when ($\tilde{W}_2 = 1$).

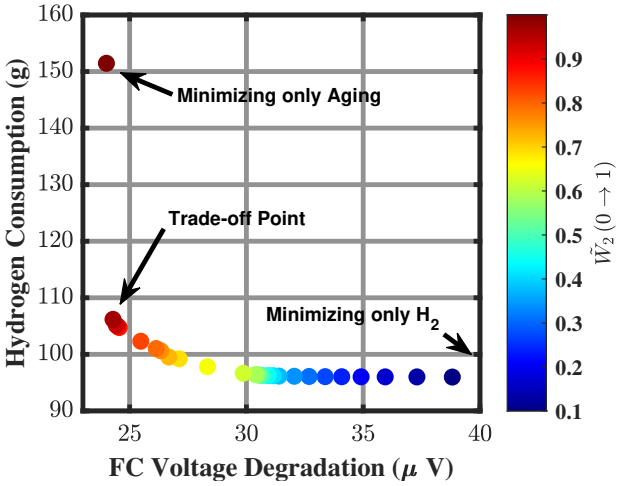

Fig. 5. Pareto front analysis on WLTP drive cycle

The Pareto curve highlights the ability of the proposed DP model to significantly minimize FC degradation while maintaining hydrogen consumption as low as possible. This behavior is achieved due to the constraints imposed on supplying power for EV traction and battery charging to precisely meet the desired terminal SOC across all weight configurations. Specifically, total FC degradation decreases as long as $\tilde{W}_2$ increases and hydrogen consumption slightly increases, except when $\tilde{W}_2$ equals one, as hydrogen consumption is no longer an objective for DP. Therefore, to minimize FC degradation during the forward simulation, the following penalty weight values are selected. These weights leverage DP's capability to limit significant increases in hydrogen consumption for all weights.

$$\tilde{W}_1 = 0.001, \quad \tilde{W}_2 = 0.999$$

4.2 Optimal Energy Management Strategy

Starting with an initial battery SOC of 50%, we present the optimization results obtained from running the forward simulation on MATLAB. The degradation-optimized controller is compared with a baseline controller that is optimized only for fuel consumption, i.e. ($\tilde{W}_2 = 0$).

The obtained forward results demonstrate that the optimal energy management strategy relies only on the battery to deliver the EV's traction power, without using the fuel cell, and depends on regenerative energy to charge the battery. This strategy avoids hydrogen usage and consequently eliminates FC degradation. However, the fuel cell must be activated when the battery SOC is low or when the traction energy exceeds the battery's capabilities, to help maintain the battery's SOC and meet the EV's power demand.

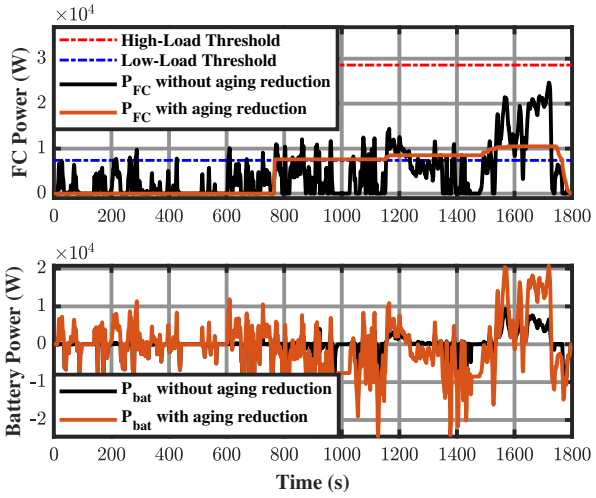

Fig. 6. Impact of selected weights on optimizing FC load profile during WLTP drive cycle

Once the FC is triggered, it should be precisely loaded to minimize voltage degradation. Since frequent start-stop cycling is the primary source of degradation, optimal loading conditions can be achieved by limiting the number of start-stop cycles to a single cycle. Additionally, degradation caused by idling and high-power demand can be avoided by operating the FC above the low-load region and below the high-load threshold. Finally, the FC must be constrained to supply constant power in order to reduce degradation caused by load fluctuations.

Implementing the FC loading strategy derived from our proposed DP reduces total FC degradation by 98.38%, extending its lifespan from 20 hours to 1235.2 hours. Meanwhile, hydrogen consumption remains approximately

unchanged, with only a slight increase of 10.91% due to limiting the FC to a single start-stop cycle.

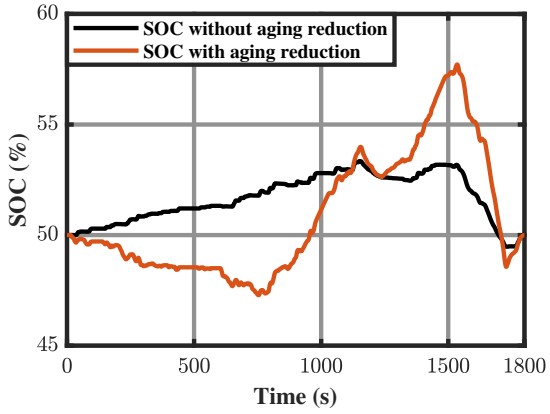

Fig. 7. Battery SOC before and after considering FC aging

Table 5. Total cost for WLTP drive cycle

Weights		Total H_2 Consumption	Total FC Degradation	Expected FC Lifetime
W_1	W_2			
1	0	95.7 (g)	1502.5 (μV)	20 (h)
0.001	0.999	106.2 (g)	24.3 (μV)	1235.2 (h)
0	1	151.5 (g)	24 (μV)	1249.7 (h)

Table 6. Total FC aging for WLTP drive cycle

Weights		Start-Stop	Load-Change	Low-Load	High-Load
W_1	W_2				
1	0	1482.4 (μV)	18.1 (μV)	1.97 (μV)	0 (μV)
0.001	0.999	23.91 (μV)	0.3 (μV)	0.1 (μV)	0 (μV)
0	1	23.91 (μV)	0.09 (μV)	0.006 (μV)	0 (μV)

5. CONCLUSION

This study presents a two-state, multi-objective DP model to determine the optimal energy management strategy for a FCHEV, minimizing both fuel consumption and FC aging. To ensure equal weighting of both objectives in the optimization process, the cost functions are normalized.

Firstly, Pareto front analysis is implemented to explore the trade-off between the weights of both objectives. Secondly, the optimal energy management strategy is developed using chosen weights from the Pareto analysis, which shows a 98.38% reduction in FC degradation and a remarkable increase in the stack's estimated lifetime. Meanwhile, hydrogen consumption remains largely unaffected, with a modest increase of 10.91%. The optimized controller focuses on reducing transient loading and limiting start-stop cycles to achieve this result.
Building on these promising results, it is recommended to evaluate the effectiveness of the derived control strategy through experimental testing. Additionally, it's crucial to investigate the impact of battery and FC sizing on the FC's optimal trajectory. Furthermore, the exploration of online EMS methods and integrating them with more accurate FC degradation models would be highly valuable.

REFERENCES

Alyakhni, A., Boulon, L., Vinassa, J.M., and Briat, O. (2021). A Comprehensive Review on Energy Management Strategies for Electric Vehicles Considering Degradation Using Aging Models. *IEEE Access*, 9, 143922–143940.

Bertsekas, D.P. (2005). *Dynamic Programming and Optimal Control*. Athena Scientific, Belmont, MA, USA.

Bressel, M., Hilairet, M., Hissel, D., and Ould Bouamama, B. (2016). Extended Kalman Filter for prognostic of Proton Exchange Membrane Fuel Cell. *Applied Energy*, 164, 220–227.

Chen, H., Pei, P., and Song, M. (2015). Lifetime prediction and the economic lifetime of Proton Exchange Membrane fuel cells. *Applied Energy*, 142, 154–163.

Fletcher, T., Thring, R., and Watkinson, M. (2016). An Energy Management Strategy to concurrently optimise fuel consumption & PEM fuel cell lifetime in a hybrid vehicle. *International Journal of Hydrogen Energy*, 41(46), 21503–21515.

Harel, F. (2021). IEEE PHM Data Challenge 2014. Fuel Cell Lab. `https://search-data.ubfc.fr/FR-18008901306731-2021-07-19_IEEE-PHM-Data-Challenge-2014.html`. Accessed: November 27, 2024.

Hu, Z., Li, J., Xu, L., Song, Z., Fang, C., Ouyang, M., Dou, G., and Kou, G. (2016). Multi-objective energy management optimization and parameter sizing for proton exchange membrane hybrid fuel cell vehicles. *Energy Conversion and Management*, 129, 108–121.

Liu, Y., Liang, J., Song, J., and Ye, J. (2022). Research on Energy Management Strategy of Fuel Cell Vehicle Based on Multi-Dimensional Dynamic Programming. *Energies*, 15(14).

Moratti, G., Villani, M., Beltrami, D., Uberti, S., Iora, P., and Tribioli, L. (2024). Optimization with Dynamic Programming of the Energy Management Strategy for a Fuel Cell Hybrid Heavy-Duty Truck Minimizing Hydrogen Consumption and Degradation. In *Conference on Sustainable Mobility*. SAE International.

Pei, P., Chang, Q., and Tang, T. (2008). A quick evaluating method for automotive fuel cell lifetime. *International Journal of Hydrogen Energy*, 33(14), 3829–3836.

Song, K., Wang, X., Li, F., Sorrentino, M., and Zheng, B. (2020). Pontryagin's minimum principle-based real-time energy management strategy for fuel cell hybrid electric vehicle considering both fuel economy and power source durability. *Energy*, 205, 118064.

Sulaiman, N., Hannan, M.A., Mohamed, A., Ker, P.J., Majlan, E.H., and Wan Daud, W.R. (2018). Optimization of energy management system for fuel-cell hybrid electric vehicles: Issues and recommendations. *Applied Energy*, 228, 2061–2079.

Teng, T., Zhang, X., Dong, H., and Xue, Q. (2020). A comprehensive review of energy management optimization strategies for fuel cell passenger vehicle. *International Journal of Hydrogen Energy*, 45(39), 20293–20303.

Yue, M., Jemei, S., Gouriveau, R., and Zerhouni, N. (2019). Review on health-conscious energy management strategies for fuel cell hybrid electric vehicles: Degradation models and strategies. *International Journal of Hydrogen Energy*, 44(13), 6844–6861.

Zhang, P., Yan, F., and Du, C. (2015). A comprehensive analysis of energy management strategies for hybrid electric vehicles based on bibliometrics. *Renewable and Sustainable Energy Reviews*, 48, 88–104.